Alternative routes for production of the drug candidate D-*chiro*-inositol with *Corynebacterium glutamicum* using endogenous or promiscuous plant enzymes

Paul Ramp, Christina Mack, Astrid Wirtz, Michael Bott[#]

IBG-1: Biotechnology, Institute of Bio- and Geosciences, Forschungszentrum Jülich, Jülich, Germany

[#]Corresponding author: m.bott@fz-juelich.de

ABSTRACT

D-*chiro*-Inositol (DCI) is a promising drug candidate for treating insulin resistance and associated diseases such as type 2 diabetes or polycystic ovary syndrome. In this study, we developed two production processes for DCI using *Corynebacterium glutamicum* as host. In the first process, *myo*-inositol (MI) is oxidized to 2-keto-*myo*-inositol (2KMI) by the inositol dehydrogenase (IDH) IolG and then isomerized to 1-keto-D-*chiro*-inositol (1KDCI) by the isomerases Cg0212 or Cg2312, both of which were identified in this work. 1KDCI is then reduced to DCI by IolG. Overproduction of IolG and Cg0212 in a chassis strain unable to degrade inositols allowed the production of 1.1 g/L DCI from 10 g/L MI. As both reactions involved are reversible, only a partial conversion of MI to DCI can be achieved. To enable higher conversion ratios, a novel route towards DCI was established by utilizing the promiscuous activity of two plant-derived enzymes, the NAD^+-dependent D-ononitol dehydrogenase MtOEPa and the NADPH-dependent D-pinitol dehydrogenase MtOEPb from *Medicago truncatula* (barrelclover). Heterologous production of these enzymes in the chassis strain led to the production of 1.6 g/L DCI from 10 g/L MI. For replacing the substrate MI by glucose, the two plant genes were co-expressed with the endogenous *myo*-inositol-1-phosphate synthase gene *ino1* either as a synthetic operon or using a novel, bicistronic T7-based expression vector. With the single operon construct, 0.75 g/L DCI was formed from 20 g/L glucose, whereas with the bicistronic construct 1.2 g/L DCI was obtained, disclosing *C. glutamicum* as an attractive host for of D-*chiro*-inositol production.

1. Introduction

D-*chiro*-Inositol (DCI) is a cyclitol ($C_6H_{12}O_6$) and one of nine different isomers of inositols besides *myo*-, *scyllo*-, *allo*-, *muco*-, *epi*-, *neo*-, L-*chiro*-, and *cis*-inositol (López-Gambero et al., 2020; Thomas et al., 2016). Together with *myo*-inositol (MI), DCI regulates several metabolic pathways and hormonal signaling in the human body and is involved in cell growth, survival, and reproduction (Chiofalo et al., 2017; Dinicola et al., 2014; Kachhawa et al., 2021; Vitale et al., 2021). As inositol phosphoglycans (IPGs), both MI and DCI (MI-IPG and DCI-IPG) function as second messengers involved in insulin signaling, with DCI-IPG being mainly involved in the regulation of glycogen synthesis and maintaining insulin sensitivity (Larner, 2002; Ortmeyer et al., 1993).

DCI is regarded as a drug candidate for the treatment of metabolic diseases linked to insulin resistance. Insulin-resistant individuals, such as those with type 2 diabetes or women with polycystic ovary syndrome (PCOS), exhibit impaired synthesis of DCI-IPG (Homburg, 2008; Larner et al., 2010). PCOS is a diverse, multifaceted disorder characterized by ovarian dysfunction, infertility, hyperandrogenism, and name-giving polycystic ovaries. Oral administration of DCI, both alone and in combination with MI, increased general insulin sensitivity in tissues of type 2 diabetes patients (Gambioli et al., 2021; Pintaudi et al., 2016) and induced ovulation in PCOS patients (Monastra et al., 2017; Ortmeyer et al., 1993).

The industrial preparation of DCI is currently achieved by removing the 3-*O*-methyl group of soybean-derived D-pinitol (DPIN) via chemical hydrolysis with a high concentration of hydrochloric or hydrobromic acid (Sanchez-Hidalgo et al., 2021). In recent years, an alternative microbial process for DCI synthesis was described. It is based on the fact that DCI was found in some bacteria, which can utilize inositols as sole carbon and energy sources, such as *Bacillus subtilis*. In this species, MI and DCI are first taken up via specific transporters and then oxidized to 2-keto-*myo*-inositol (2KMI) and 1-keto-D-*chiro*-inositol (1KDCI), respectively, by the inositol dehydrogenase (IDH) IolG in a reversible NAD^+-dependent reaction (Yoshida et al.,

2006). The inososе isomerase IolI is then responsible for the reversible interconversion of 1KDCI to 2KMI, which is metabolized in an inositol-specific catabolic pathway forming acetyl-CoA and dihydroxyacetone phosphate (Yoshida et al., 2006; Yoshida et al., 2008). IolI has a TIM barrel fold and structural similarity to both endonuclease IV and xylose isomerase (Yoshida et al., 2006). Enzymatic assays with purified IolI showed a reaction equilibrium with a molar ratio of 77:23 in favor of 2KMI. With an engineered *B. subtilis* strain unable to degrade inositols and overexpressing *iolG* and *iolI*, the production of DCI from MI with a yield of 6% was achieved (Yoshida et al., 2006).

Corynebacterium glutamicum is a soil-dwelling actinobacterium that is used as an industrial cell factory, in particular for large-scale production of L-glutamate and L-lysine (Becker et al., 2018; Eggeling and Bott, 2015; Hermann, 2003; Wendisch, 2020; Wolf et al., 2021). It can use MI as sole carbon source (Klaffl et al., 2013; Krings et al., 2006). In a recent study, we reported that *C. glutamicum* can grow not only with MI, but also with *scyllo*-inositol (SI) and DCI as sole carbon and energy source, similar to *B. subtilis* (Ramp et al., 2022). The two IDHs IolG and OxiD were shown to catalyze the NAD^+-dependent oxidation of DCI, however, no IolI-type inososе isomerase that interconverts 1KDCI to 2KMI has been identified in *C. glutamicum* so far. In contrast to *B. subtilis*, *C. glutamicum* is not only able to degrade inositols, but also has the intrinsic capability to synthesize MI in two steps from glucose 6-phosphate, which makes it an attractive host for the production of inositols from cheap carbon sources (Baumgart et al., 2013) . We recently demonstrated this potential by developing *C. glutamicum* strains that efficiently produce SI from glucose and sucrose (Ramp et al. 2021).

This study aimed at the engineering of *C. glutamicum* strains for the production of DCI. In that context, we searched for endogenous isomerases catalyzing the conversion of 1KDCI to 2KMI to utilize them for DCI synthesis and identified three enzymes displaying this activity, Cg0212, Cg2312, and Cg3390. Overproduction of IolG together with Cg0212 in the chassis strain *C. glutamicum* MB001(DE3)ΔIOL, which is unable to catabolize inositols, allowed the

production of DCI from MI with a yield of up to 18% (with respect to consumed MI). Beyond this endogenous pathway, we identified and implemented a novel alternative route for production of DCI from MI, which is based on the substrate promiscuity of two plant enzymes, the NAD^+-dependent D-ononitol dehydrogenase MtOEPa and the $NADP^+$-dependent D-pinitol dehydrogenase MtOEPb from *Medicago truncatula* (barrelclover). Using this pathway, also DCI production from glucose was achieved.

2. Materials and methods

2.1 Bacterial strains, plasmids and growth conditions

All bacterial strains and plasmids used in this work are listed in Table 1. All cloning steps were performed with *Escherichia coli* DH5α as host. *E. coli* strains were cultivated at 37 °C on LB agar plates or in lysogeny broth (LB) (Bertani, 1951) with 50 µg/mL kanamycin when appropriate. For growth studies, *C. glutamicum* was cultivated in a BioLector microcultivation system (m2p-labs, Baesweiler, Germany). Single colonies were transferred in BHI medium and cultivated for 8 h at 30 °C as a first preculture. The second preculture in defined CGXII medium (Keilhauer et al., 1993) with 0.03 g/L protocatechuic acid as iron chelator and 20 g/L glucose was inoculated with 10% of the first preculture and cultivated for 16 h at 30 °C. Before inoculation of the main cultures, cells were washed once with CGXII medium without a carbon source. BioLector cultivations were performed in 800 µL CGXII medium containing 1% (wt/vol) of the desired carbon source in 48-well FlowerPlates (m2p-labs, Baesweiler, Germany) at 1200 rpm and 30 °C. Growth was measured online as scattered light at 620 nm (Kensy et al., 2009). For protein production, *C. glutamicum* was cultivated in 200 mL BHI medium supplemented with 2% (wt/vol) glucose in 2 L baffled shake flasks at 100 rpm and 30°C. For inositol production experiments, *C. glutamicum* was cultivated in 50 mL CGXII medium supplemented with 20 g/L glucose and for DCI production with 10 g/L MI in 500 mL baffled shake flasks at 30 °C and 130 rpm for 72 h. When appropriate, 25 µg/mL kanamycin was added

to the medium. Gene expression was induced by addition of isopropyl-β-D-thiogalactoside (IPTG) at the indicated concentrations. Bacterial growth in shake flasks was followed by measuring the optical density at 600 nm (OD_{600}) using an Ultrospec 2100 pro photometer (Biochrom).

2.2 Recombinant DNA work and construction of deletion mutants

All plasmids and oligonucleotides used in this study are listed in Table 1 and Table S1, respectively. PCRs, DNA restrictions, and plasmid constructions were performed according to established protocols (Gibson et al., 2009; Green et al., 2012). DNA sequencing and oligonucleotide synthesis were performed by Eurofins Genomics (Ebersberg, Germany). Chemically competent *E. coli* cells were transformed according to an established protocol (Hanahan, 1983). *C. glutamicum* was transformed via electroporation as described previously (van der Rest et al., 1999). *C. glutamicum* MB001(DE3) deletion mutants were constructed via double homologous recombination as described previously (Niebisch and Bott, 2001) using pK19mobsacB-derived plasmids. The chromosomal deletions were confirmed via colony-PCR using oligonucleotides annealing outside of the deleted region. For protein overproduction and purification, genes were cloned into the recently described pPREx6 plasmid (Ramp et al., 2022) downstream of the T7 promoter and upstream of a Strep-Tag II encoding sequence. For the construction of the pMKEx2-based expression plasmids, the corresponding target genes were cloned downstream of the *C. glutamicum* consensus ribosome binding site (RBS) via Gibson assembly. For construction of the bicistronic expression plasmid pMKEx2BiT7, we amplified the T7 promoter, the second multiple cloning site (MCS), and the corresponding terminator from plasmid pETDuet-1 using the oligonucleotides P72 and P73 and joined them with the pMKEx2 backbone amplified with the oligonucleotides P74xP75 and P76x77 (Table S1) via Gibson assembly**.** The DNA sequences of the *MtOEPa* and *MtOEPb* genes were codon-optimized for *C. glutamicum* and ordered as DNA strings from ThermoFisher Scientific.

2.3 Protein overproduction and purification

C. glutamicum MB001(DE3) was transformed with pPREx6-based expression plasmids for inositol dehydrogenase production and cultivated in 200 mL BHI medium supplemented with 20 g/L glucose. Overexpression of the target genes was induced with 250 µM IPTG after 3 h and cells were harvested after 24 h of cultivation via centrifugation at 5,000 g for 20 min at 4 °C. Cell pellets were washed and resuspended in 4 mL lysis buffer (100 mM KPO_4 pH 7.5, 150 mM NaCl, 1 mM $MgSO_4$) per g cell wet weight and lysed by five passages through a French Press at 124 MPa. The resulting cell extract was first centrifuged at 5,000 g and 4 °C for 20 min and the supernatant was then subjected to ultracentrifugation at 45,000 g and 4 °C for 1 h. The resulting supernatant was incubated with avidin (25 µg/mg protein) for 30 min on ice before performing purification on an Äkta pure protein purification system (Cytiva) via StrepTactin Sepharose affinity chromatography and subsequent size exclusion chromatography.

A StrepTrap HP 1 mL column (GE Healthcare) was equilibrated with binding buffer (100 mM KPO_4 pH 7.5, 150 mM NaCl, 1 mM $MgSO_4$) before loading the avidin-treated protein extract. The column was washed with 10 column volumes (CV) of binding buffer and bound proteins were then eluted in six 0.5 ml fractions with elution buffer I (100 mM KPO_4 pH 7.5, 150 mM NaCl, 1 mM $MgSO_4$, 2.5 mM desthiobiotin). The protein-containing elution fractions were combined and concentrated by using a 10 kDa AMICON filter and centrifuging at 3,500 g and 4 °C to a final volume of 500 µL. The concentrated protein was then applied to a Superdex 200 Increase size exclusion chromatography column (GE Healthcare) that had been equilibrated with 2 CV of elution buffer II (100 mM KPO_4 pH 7.5, 1 mM $MgSO_4$). Protein was eluted with 1.5 CV of elution buffer II and collected in 2 mL fractions. The purity and the apparent molecular mass of the proteins after both purification steps were determined by SDS-PAGE with 12% (wt/vol) separating gels followed by Coomassie staining according to standard procedures (Green et al., 2012). Protein concentrations were determined using the Bradford

assay (Coomassie blue G-250) and measuring concentration-dependent blue coloration at 595 nm (Thermofisher Scientific).

2.4 In vitro MI-DCI interconversion studies

To analyze inososе isomerase activity *in vitro*, 50 µg of purified inososе isomerase was combined with 50 µg of purified IolG in 200 µL reaction buffer containing 50 mM potassium phosphate buffer pH 7.5, 1 mM $MgSO_4$, 0.1 mM $MnSO_4$, 5 mM NAD^+, and either 10 g/L MI (55.51 mM) or 10 g/L DCI (55.51 mM). The reaction was incubated at 30 °C for 16 h and stopped via heating at 85 °C for 15 min. For inositol analysis, the samples were subjected to HPLC analysis.

2.5 Inositol analysis by HPLC

1 mL culture was centrifuged at 17,000 g for 20 min, the supernatant was filtered (0.2 µm syringe filter, Whatman™, GE Healthcare, Freiburg, Germany) and frozen at -20 °C until further analysis. Thawed samples were diluted 1:1 with deionized water and used for HPLC analysis. A 5 µL sample was measured using an Agilent LC-1100 system (Agilent, Santa Clara, CA, USA) equipped with a Carbo-Pb Guard Catridge (Phenomenex, Aschaffenburg, Germany) and a Rezex RPM-Monosaccharide 300 × 7.8 mm column (Phenomenex, Aschaffenburg, Germany). Separation was performed at 85 °C with water as eluent at a flow rate of 0.6 mL/min. Sugar and sugar alcohols were detected with a refraction index detector operated at 35 °C. The linear range lies between 0.1 g/L and 20 g/L. The retention times were 21 min for DCI and 24 min for MI.

3. Results and discussion

3.1 Identification of enzymes with inosose isomerase activity in C. glutamicum

The two inositol clusters *iol1* and *iol2* contain three genes encoding putative sugar phosphate isomerases, i.e. *iolH* (cg0205), cg0212, and cg3390 (Fig. 1A). All three proteins showed a sequence identity of 27-29% over a query cover of 20-54% to IolI of *B. subtilis*. Cg3390 was previously identified to be active on 2KMI, converting it to yet unknown, brown-colored compounds (Ramp et al. 2021). In order to analyze if any of these three putative isomerases enable the interconversion of MI and DCI, we fused IolH, Cg0212, Cg3390 and the IDH IolG to a C-terminal Strep-Tag II and purified each protein after overproduction in *C. glutamicum* MB001(DE3) by StrepTactin Sepharose affinity chromatography followed by size-exclusion chromatography (Fig. S1). Each isomerase was tested *in vitro* for production of DCI or MI in the presence or absence of IolG with either MI or DCI as substrate, as described in Materials and Methods.

No inositol interconversion was detected in all reaction mixtures containing only one enzyme and in the reaction mixtures containing IolG and IolH, showing that IolH does not catalyze the conversion of 2KMI to 1KDCI. In contrast, when using 10 g/L MI as substrate, IolG in combination with Cg0212 led to the formation of 0.55 g/L DCI after 16 h (Fig. 1B). When starting from 10 g/L DCI, this enzyme combination produced up to 3 g/L MI, indicating that this is the favored direction (Fig. 1C). In these reactions, the reduction of the keto-intermediate by IolG recovers NAD^+, which results in a cyclic reaction until equilibrium is reached. Also the combination of IolG with Cg3390 enabled the conversion of MI to DCI, but in this case, only 0.2 g/L DCI were formed from 10 g/L MI after 16 h. In the opposite direction, nearly 1.0 g/L MI were synthesized from 10 g/L DCI, confirming this direction to be the favored one (Fig. 1C). In both reaction mixtures containing IolG and Cg3390, much more substrate (7 – 8 g/L) disappeared than product was formed and the samples showed a brown coloration (Fig. S2A), suggesting that the keto intermediates were converted to other, yet unknown

products with concomitant oxidation of NADH. In our previous studies, brown coloration was also observed *in vivo***,** when IolG and Cg3390 were overproduced in *C. glutamicum* in the presence of MI (Ramp et al., 2021).

3.2 Establishment of a DCI production process from MI based on endogenous enzymes

With Cg0212 identified as a functional isomerase enabling the conversion from MI to DCI, we aimed for a microbial DCI production process with an engineered *C. glutamicum* strain that is unable to degrade inositols. We previously constructed *C. glutamicum* MB001(DE3)Δ*iol1*Δ*iol2*, in which the gene clusters cg0196-cg0212 (*iol1*) and cg3389-cg3392 (*iol2*) were deleted (Fig. 1A) (Ramp et al., 2021). We now additionally deleted the *idhA3* gene (cg2313) encoding another putative inositol dehydrogenase, yielding the chassis strain *C. glutamicum* MB001(DE3)ΔIOL. For production of DCI, *iolG* and cg0212 were cloned as synthetic operon into the expression plasmid pMKEx2, which allows strong, inducible gene expression under the control of the T7 promoter. As controls, *iolG* and cg0212 were cloned separately into pMKEx2. The resulting plasmids pIolG-Cg0212, pIolG, and pCg0212 were introduced into *C. glutamicum* MB001(DE3)ΔIOL. A strain harboring pMKEx2 without insert served as an additional negative control.

All strains were cultivated for 72 h at 30 °C in CGXII medium with 20 g/L glucose for biomass formation and 10 g/L MI as substrate for DCI synthesis. Overexpression of *iolG* and cg0212 led to the consumption of 6 g/L MI with formation of 1.1 g/L DCI in 48 h, corresponding to a yield of 18% with respect to the consumed MI (Fig. 2). We speculate that an altered availability of NAD^+ and NADH due to metabolization of glucose contributes to the higher DCI yield obtained with the *in vivo* system compared to the *in vitro* system described above. Additionally, import and export of MI, DCI, and the keto intermediates could also contribute to the higher yield. Expression of *iolG* alone resulted in the consumption of 5 g/L MI, which was probably converted to keto intermediates, as indicated by the yellow media

coloration (Fig. S2B) that had also been observed previously for strains accumulating 2KMI (Ramp et al., 2021). To our surprise, also 0.5 g/L DCI was formed by overexpression of *iolG* alone. As cg0212 and cg3390 as well as *iolH* are deleted in *C. glutamicum* MB001(DE3)ΔIOL, this result hinted towards the presence of yet another enzyme with inosose isomerase activity encoded in the genome of *C. glutamicum*.

When performing a PSI-BLAST search (Altschul et al., 1997) with IolI of *B. subtilis* as template the best hit was the 3-dehydroshikimate dehydratase QsuB (Cg0502) of *C. glutamicum*. IolI (278 amino acids) had 26 % sequence identity to the N-terminal half of QsuB (618 amino acids). QsuB catalyzes the dehydration of 3-dehydroshikimate to protocatechuate (3,4-dihydroxybenzoate) (Kallscheuer et al., 2016; Kubota et al., 2014). To investigate if QsuB is involved in DCI formation by catalyzing the conversion of 2KMI to 1KDCI, we deleted the corresponding gene in *C. glutamicum* MB001(DE3)ΔIOL and analyzed DCI formation from MI after plasmid-based overexpression of *iolG*. As negative control, we transformed *C. glutamicum* MB001(DE3)ΔIOL with the pMKEx2 empty vector. All strains were again cultivated in CGXII medium with 20 g/L glucose and 10 g/L MI at 30°C for 72 h. MI and DCI titers were measured at the end of the cultivation. The deletion of *qsuB* had no effect on DCI formation in comparison to the parental strain MB001(DE3)ΔIOL (Fig. 3A), both strains produced up to 0.65 g/L DCI, indicating that QsuB is not the remaining inosose isomerase.

As a next step to search for inosose isomerases in *C. glutamicum*, we used the InterPro database (Blum et al., 2021) to identify proteins belonging to the xylose isomerase-like superfamily, to which IolI of *B. subtilis* belongs. For *C. glutamicum* ATCC13032, nine proteins (Table 2) are classified into this superfamily. Among the identified proteins are the isomerases IolH, Cg0212, Cg3390, and QsuB described above and the inositol dehydratase IolE, which catalyzes the dehydration of 2KMI to D-2,3-diketo-4-deoxy-*epi*-inositol (Yoshida et al., 2004). The other identified proteins include the conserved hypothetical protein Cg2917, the putative sugar phosphate isomerase Cg2822, and the two putative hydroxypyruvate isomerases Hyi

(Cg2716) and Cg2312. It is noteworthy that the cg2312 gene seems to be organized in an operon with cg2313 encoding the putative inositol dehydrogenase IdhA3 (Ramp et al., 2022). We further focused on Cg2312, Cg2716, Cg2822, and Cg2917 since *iolE*, *iolH*, cg0212, and cg3390 are already deleted in *C. glutamicum* MB001(DE3)ΔIOL and QsuB had been excluded. Individual deletion strains of MB001(DE3)ΔIOL lacking either cg2312, cg2716, cg2822, or cg2917 were constructed, transformed with pIolG, and analyzed for DCI production after 72 h (Fig. 3A). All strains reached the same final OD of about 30. Only the deletion of cg2312 led to a significantly decreased DCI titer of 0.37 g/L, while all other strains accumulated 0.65 g/L DCI.

To rule out that the combined activity of the identified putative isomerases Cg2312, Cg2716, Cg2822, Cg2917, and QsuB is responsible for the residual DCI formation, we deleted all corresponding genes in *C. glutamicum* MB001(DE3)ΔIOL. The resulting strain MB001(DE3)ΔIOLΔISO was transformed with pMKEx2, pIolG, and pMKEx2 plasmids containing *iolG* and an isomerase gene in a synthetic operon. All strains were cultivated in CGXII with 2% (w/v) glucose and 1% (w/v) MI to analyze DCI production. Consistent with the previous experiments, only MB001(DE3)ΔIOLΔISO expressing *iolG* with either cg0212 or cg2312 showed elevated DCI production (~0.6 g/L) (Fig. 3B). Strain MB001(DE3)ΔIOLΔISO pIolG-cg0212 reached only 50% of the DCI titer of strain MB001(DE3)ΔIOL pIolG-cg0212 (Fig. 2), suggesting that the expression of both cg2312 and cg0212 contributes to the production of 1.1 g/L DCI from 10 g/L MI in the latter strain. Strain MB001(DE3)ΔIOLΔISO expressing only *iolG* or *iolG* plus any other tested putative inosose isomerase gene showed a DCI production of only about 0.3 g/L. As DCI formation was still observed in strain MB001(DE3)ΔIOLΔISO pIolG, at least one other inosose isomerase seems to be present in *C. glutamicum*.

To further test this hypothesis, we analyzed the growth on DCI of a *C. glutamicum* strain in which we deleted all identified inosose isomerase genes in the recently constructed mutant *C.*

glutamicum MB001(DE3)ΔIDH, which lacks all seven IDH genes and is unable to grow on DCI (Ramp et al., 2022). The resulting deletion strain was named *C. glutamicum* MB001(DE3)ΔIDHΔISO and transformed with pMKEx2, pIolG, and pIolG-cg0212 to analyze if only IolG or an additional inososе isomerase is necessary to enable growth on DCI. As positive control, *C. glutamicum* MB001(DE3) transformed with pMKEx2-eyfp was used. The strains were cultivated in CGXII medium with 10 g/L DCI as sole carbon source in a BioLector cultivation system at 30 °C for 72 h. Gene expression was induced by addition of 20 µM IPTG at the start of the cultivation and IPTG had also been added to the overnight preculture, for which CGXII medium with 20 g/L glucose was used. The expression of *iolG* alone was sufficient to restore growth of strain MB001(DE3)ΔIDHΔISO to the wild-type level (Fig. 3C). Expression of cg0212 together with *iolG* did not result in any difference compared to the strain expressing *iolG* alone. This suggests the presence of another inososе isomerase, which interconverts 1KDCI to 2KMI. An alternative possibility is that for growth on DCI no additional inososе isomerase is necessary. The inositol dehydratase IolE, which catalyzes the dehydration of 2KMI to yield 3D-(3,5/4)-trihydroxy-cyclohexane-1,2-dione (THcHDO) (Yoshida et al., 2004), the second intermediate in the inositol catabolic pathway, was never analyzed for activity for other keto-inositol intermediates. If IolE also accepts 1KDCI as substrate, an inososе isomerase is not required for growth on DCI. Further studies are required to test this possibility.

3.3 Establishment of a novel DCI production route in C. glutamicum based on the substrate promiscuity of two plant enzymes

The DCI production process described above with a yield of 18% from MI is based on the unfavorable reduction of 1KDCI to DCI with NADH (Fig. 1B). To achieve high DCI production titers high concentrations of MI would be required and process regimes with *in situ* product removal, which, however, might be difficult for the isomers MI and DCI. We therefore searched for an alternative DCI production route that shifts the equilibrium in favor of DCI production.

In plants, DCI is mainly found as the 3-*O*-methylated derivative D-pinitol (DPI) (3-*O*-methyl-D-*chiro*-inositol), which is synthesized from MI. MI is first methylated by an inositol methyl transferase (IMT) resulting in D-ononitol (ONO, 4-*O*-methyl-*myo*-inositol), which then is converted to D-pinitol (Loewus and Murthy, 2000). Recently, a two-step D-ononitol epimerization pathway was identified in *Medicago truncatula* (Pupel et al., 2019). In the first step, ONO is oxidized by the NAD^+-dependent dehydrogenase MtOEPa to 4-*O*-methyl-D-*myo*-1-inososе. In the second step, the keto intermediate is reduced to DPI by the NADPH-dependent dehydrogenase MtOEPb (Fig. 4 A). As the only difference between ONO and MI and between DPI and DCI is a single methyl group, we wondered whether the two dehydrogenases MtOEPa and MtOEPb might also accept MI and 1KDCI as substrates, respectively (Fig. 4B). Such a conversion would enable to drive the reaction towards DCI, as the cellular ratios of NAD^+/NADH and $NADP^+$/NADPH are usually in favor of NAD^+ and NADPH with absolute concentrations depending on the organism and growth conditions (Amador-Noguez et al., 2011; Andersen and von Meyenburg, 1977; Bennett et al., 2009; Spaans et al., 2015).

To test this possibility, we cloned the codon-optimized *MtOEPa* and *MtOEPb* genes as synthetic operons with different gene orders (*MtOEPa-b* and *MtOEPb-a*) and each gene individually in pMKEx2. The resulting plasmids were introduced into *C. glutamicum* MB001(DE3)ΔIOLΔISO and production of DCI from MI was analyzed as described above. Production was compared to strain MB001(DE3)ΔIOL pIolG-cg0212. The expression of both plant-derived dehydrogenases indeed enabled the formation of DCI (Fig. 4C). Strain MB001(DE3)ΔIOLΔISO pOEPa-b accumulated up to 1.6 g/L DCI from 2 g/L consumed MI (80% yield), whereas strain MB001(DE3)ΔIOLΔISO pOEPb-a formed only 0.5 g/L DCI from 0.7 g/L consumed MI (71% conversion), showing that the gene order was relevant. *C. glutamicum* MB001(DE3)ΔIOL pIolG-cg0212 again reached ~1.1 g/L DCI from 6 g/L consumed MI (18% yield), indicating that the novel pathway based on MtOEPa and MtOEPb is more efficient than the one based on endogenous enzymes.

3.4 Production of DCI from glucose with C. glutamicum

Using the new DCI production route based on MtOEPa and MtOEPb, we also aimed for production of DCI from glucose, which is a cheaper carbon source than MI. In a recent study, we established production of SI from glucose and sucrose utilizing the innate ability of *C. glutamicum* to synthesize MI from glucose 6-phosphate via the *myo*-inositol-1-phosphate synthase Ino1 followed by dephosphorylation via an inositol monophosphatase (Ramp et al., 2021). By overexpressing the *ino1* gene together with the inositol dehydrogenase genes *iolG* and *iolW* production of SI from sucrose and glucose was achieved (Ramp et al., 2021).

We cloned the *MtOEPa* and *MtOEPb* genes in a synthetic operon with *ino1* into pMKEx2 and introduced the resulting plasmid pInoDCI (Fig. 5A) into *C. glutamicum* MB001(DE3)ΔIOLΔISO. The resulting strain was cultivated in CGXII medium with 20 g/L glucose for 72 h at 30 °C in comparison to strains expressing only *ino1* (pIno) or containing an empty vector. Gene expression was induced by 500 µM IPTG added three hours after start of the cultivation. Strain MB001(DE3)ΔIOLΔISO pIno produced up to 1.8 g/L MI, confirming that overexpression of *ino1* leads to MI overproduction and secretion. Strain MB001(DE3)ΔIOLΔISO pInoDCI accumulated up to 0.75 g/L DCI and 0.65 g/L MI after 72 h (Fig. 5B), summing up to 1.40 g/L inositols. The accumulation of MI hinted towards a limitation in the conversion of MI to DCI by MtOEPa and MtOEPb.

The gene order in synthetic operons resulting in polycistronic mRNAs encoding biochemical pathways is of relevance for optimally tuned gene expression. Translation initiation levels decrease with increasing distance to the transcriptional start (Lim et al., 2011). We assumed that expression especially of the *MtOEPb* gene in plasmid pInoDCI is insufficient for optimal DCI formation. To improve expression of the genes for MtOEPa and MtOEPb, but also retain a high expression level of *ino1*, we constructed a new pMKEx2 expression plasmid allowing for bicistronic, inducible gene expression under the control of two T7 promoters. There are

365 already several examples of bicistronic expression vectors developed for *C. glutamicum*
366 (Gauttam et al., 2019; Goldbeck and Seibold, 2018; Liu et al., 2017), yet there is no plasmid
367 available containing two T7 promoters that would allow strong expression in *C. glutamicum*
368 MB001(DE3). We amplified an expression cassette encoding the T7 promoter, a multiple
369 cloning site including a ribosome binding site plus a NdeI restriction site, and a terminator from
370 the bicistronic expression plasmid pETDuet-1 and cloned this cassette in opposite direction to
371 the original T7 promoter of pMKEx2, yielding the bicistronic expression plasmid pMKEx2-
372 BiT7 (Fig. 5A). We then cloned *ino1* under the control of the first and *MtOEPa-b* under the
373 control of the second T7 promoter yielding the bicistronic plasmid pBiT7-InoDCI (Fig. 5A).
374 When cultivated in CGXII medium with 20 g/L glucose, *C. glutamicum*
375 MB001(DE3)ΔIOLΔISO transformed with pBiT7-InoDCI formed 1.2 g/L DCI and 0.23 g/L
376 MI after 72 h (Fig. 5B), showing that bicistronic expression increased DCI production by 60 %
377 and simultaneously decreased MI accumulation by 38 %.
378
379 **4. Conclusions**
380 We previously established *C. glutamicum* as a suitable host for the biotechnological
381 production of SI, a drug candidate against Alzheimer's disease. In this study, we constructed
382 *C. glutamicum* strains that enable the biotechnological production of another pharmacologically
383 highly interesting inositol isomer, D-*chiro*-inositol. We identified the three inositol isomerases
384 Cg0212, Cg2312, and Cg3390 in *C. glutamicum* that enable the interconversion of 2KMI to
385 1KDCI. We therefore suggest to name the corresponding genes *iolI1* (cg0212), *iolI2* (cg2312),
386 and *iolI3* (cg3390) following the nomenclature in *B. subtilis*. Overexpression of cg0212
387 together with *iolG* led to DCI production from MI with yields of up to 18%. The yield of this
388 process is limited by the reversibility of the involved reactions and the use of NADH for
389 reducing 1KDCI to DCI by IolG. Utilizing the promiscuous activity of the NAD^+-dependent
390 D-ononitol dehydrogenase MtOEPa and the $NADP^+$-dependent D-pinitol dehydrogenase

MtOEPb of the plant *M. trunculata*, we established an alternative production route for DCI from MI enabling yield of up to 80%. This pathway was additionally used to produce DCI from the cheaper substrate glucose by simultaneous overproduction of the Ino1 enzyme. As conversion of the intermediate MI to DCI was limiting and led to accumulation of MI, a novel bicistronic expression plasmid was used for expression of *ino1* and *MtOEPa-b* from separate T7 promoters. This enabled a significant increase of DCI production with simultaneous reduction of MI accumulation, enabling a yield of 6% DCI from glucose. As there is an increasing interest in the use of inositols for pharmacological applications, cheap and efficient biotechnological production processes are highly desirable. Our studies showed that *C. glutamicum* has the potential to serve as a suitable host for the industrial production of DCI, SI, and MI. Future studies should be directed to further strain and enzyme optimization and bioprocess development including downstream processing.

Declaration of competing interest

PR and MB have a patent pending for DCI production. The remaining authors have no conflicts of interest to declare.

Acknowledgements

This project was financially supported by the CLIB-Competence Center Biotechnology (CKB) funded by the European Regional Development Fund ERDF [grant number 34.EFRE-0300097] and by the German Federal Ministry of Education and Research (BMBF) [grant number 031B0918A], as part of the innovation lab „AutoBiotech“ within the project “BioökonomieREVIER”.

Author statement

Paul Ramp: Conceptualization, Methodology, Investigation, Writing – Initial Draft, Visualization. Christina Mack: Investigation. Astrid Wirtz: Methodology, Investigation. Michael Bott: Conceptualization, Supervision, Writing – review & editing, Funding acquisition.

References

Altschul, S. F., Madden, T. L., Schäffer, A. A., Zhang, J., Zhang, Z., Miller, W., Lipman, D. J., 1997. Gapped BLAST and PSI-BLAST: a new generation of protein database search programs. Nucleic Acids Res. 25**,** 3389-3402.

Amador-Noguez, D., Brasg, I. A., Feng, X.-J., Roquet, N., Rabinowitz, J. D., 2011. Metabolome remodeling during the acidogenic-solventogenic transition in *Clostridium acetobutylicum*. Appl. Environ. Microbiol. 77**,** 7984-7997.

Andersen, K. B., von Meyenburg, K., 1977. Charges of nicotinamide adenine nucleotides and adenylate energy charge as regulatory parameters of the metabolism in *Escherichia coli*. J. Biol. Chem. 252**,** 4151-4156.

Baumgart, M., Luder, K., Grover, S., Gätgens, C., Besra, G. S., Frunzke, J., 2013. IpsA, a novel LacI-type regulator, is required for inositol-derived lipid formation in *Corynebacteria* and *Mycobacteria*. BMC Biol. 11**,** 122.

Becker, J., Rohles, C. M., Wittmann, C., 2018. Metabolically engineered *Corynebacterium glutamicum* for bio-based production of chemicals, fuels, materials, and healthcare products. Metab. Eng. 50**,** 122-141.

Bennett, B. D., Kimball, E. H., Gao, M., Osterhout, R., Van Dien, S. J., Rabinowitz, J. D., 2009. Absolute metabolite concentrations and implied enzyme active site occupancy in *Escherichia coli*. Nat. Chem. Biol. 5**,** 593-599.

Bertani, G., 1951. Studies on lysogenesis. The mode of phage liberation by lysogenic *Escherichia coli*. J. Bacteriol. 62**,** 293-300.

Blum, M., Chang, H. Y., Chuguransky, S., Grego, T., Kandasaamy, S., Mitchell, A., Nuka, G., Paysan-Lafosse, T., Qureshi, M., Raj, S., Richardson, L., Salazar, G. A., Williams, L., Bork, P., Bridge, A., Gough, J., Haft, D. H., Letunic, I., Marchler-Bauer, A., Mi, H., Natale, D. A., Necci, M., Orengo, C. A., Pandurangan, A. P., Rivoire, C., Sigrist, C. J. A., Sillitoe, I., Thanki, N., Thomas, P. D., Tosatto, S. C. E., Wu, C. H., Bateman, A., Finn, R. D., 2021. The InterPro protein families and domains database: 20 years on. Nucleic Acids Res. 49**,** D344-D354.

Chiofalo, B., Laganà, A. S., Palmara, V., Granese, R., Corrado, G., Mancini, E., Vitale, S. G., Frangež, H. B., Vrtačnik-Bokal, E., Triolo, O., 2017. Fasting as possible complementary approach for polycystic ovary syndrome: Hope or hype? Med. Hypotheses 105**,** 1-3.

Dinicola, S., Chiu, T. T., Unfer, V., Carlomagno, G., Bizzarri, M., 2014. The rationale of the *myo*-inositol and D-*chiro*-inositol combined treatment for polycystic ovary syndrome. J. Clin. Pharmacol. 54**,** 1079-1092.

Eggeling, L., Bott, M., 2015. A giant market and a powerful metabolism: L-lysine provided by *Corynebacterium glutamicum*. Appl. Microbiol. Biotechnol. 99**,** 3387-3394.

Gambioli, R., Forte, G., Aragona, C., Bevilacqua, A., Bizzarri, M., Unfer, V., 2021. The use of D-*chiro*-Inositol in clinical practice. Eur. Rev. Med. Pharmacol. Sci. 25**,** 438-446.

Gauttam, R., Desiderato, C., Jung, L., Shah, A., Eikmanns, B. J., 2019. A step forward: Compatible and dual-inducible expression vectors for gene co-expression in *Corynebacterium glutamicum*. Plasmid 101**,** 20-27.

Gibson, D. G., Young, L., Chuang, R. Y., Venter, J. C., Hutchison, C. A., 3rd, Smith, H. O., 2009. Enzymatic assembly of DNA molecules up to several hundred kilobases. Nat. Methods 6**,** 343-345.

Goldbeck, O., Seibold, G. M., 2018. Construction of pOGOduet–an inducible, bicistronic vector for synthesis of recombinant proteins in *Corynebacterium glutamicum*. Plasmid 95**,** 11-15.

Green, M. R., Hughes, H., Sambrook, J., MacCallum, P., 2012. Molecular cloning: a laboratory manual. Cold Spring Harbor Laboratory Press, Cold Spring Harbor, New York.

Hanahan, D., 1983. Studies on transformation of *Escherichia coli* with plasmids. J. Mol. Biol. 166**,** 557-580.

Hermann, T., 2003. Industrial production of amino acids by coryneform bacteria. J. Biotechnol. 104**,** 155-172.

Homburg, R., 2008. Polycystic ovary syndrome. Best Pract. Res. Cl. Ga. 22**,** 261-274.

Kachhawa, G., Senthil Kumar, K. V., Kulshrestha, V., Khadgawat, R., Mahey, R., Bhatla, N., 2021. Efficacy of *myo*-inositol and D-*chiro*-inositol combination on menstrual cycle regulation and

improving insulin resistance in young women with polycystic ovary syndrome: A randomized open-label study. Int. J. Gyncecol. Obstet. 158**,** 278-284.
Kallscheuer, N., Vogt, M., Stenzel, A., Gätgens, J., Bott, M., Marienhagen, J., 2016. Construction of a *Corynebacterium glutamicum* platform strain for the production of stilbenes and (2S)-flavanones. Metab. Eng. 38**,** 47-55.
Keilhauer, C., Eggeling, L., Sahm, H., 1993. Isoleucine synthesis in *Corynebacterium glutamicum*: molecular analysis of the *ilvB-ilvN-ilvC* operon. J. Bacteriol. 175**,** 5595-5603.
Kensy, F., Zang, E., Faulhammer, C., Tan, R. K., Büchs, J., 2009. Validation of a high-throughput fermentation system based on online monitoring of biomass and fluorescence in continuously shaken microtiter plates. Microb. Cell Fact. 8**,** 31.
Klaffl, S., Brocker, M., Kalinowski, J., Eikmanns, B. J., Bott, M., 2013. Complex regulation of the phosphoenolpyruvate carboxykinase gene pck and characterization of its GntR-type regulator IolR as a repressor of *myo*-inositol utilization genes in *Corynebacterium glutamicum*. J. Bacteriol. 195**,** 4283-4296.
Kortmann, M., Kuhl, V., Klaffl, S., Bott, M., 2015. A chromosomally encoded T7 RNA polymerase-dependent gene expression system for *Corynebacterium glutamicum*: construction and comparative evaluation at the single-cell level. Microb. Biotechnol. 8**,** 253-265.
Krings, E., Krumbach, K., Bathe, B., Kelle, R., Wendisch, V. F., Sahm, H., Eggeling, L., 2006. Characterization of *myo*-inositol utilization by *Corynebacterium glutamicum*: the stimulon, identification of transporters, and influence on L-lysine formation. J. Bacteriol. 188**,** 8054-8061.
Kubota, T., Tanaka, Y., Takemoto, N., Watanabe, A., Hiraga, K., Inui, M., Yukawa, H., 2014. Chorismate-dependent transcriptional regulation of quinate/shikimate utilization genes by LysR-type transcriptional regulator QsuR in *Corynebacterium glutamicum*: carbon flow control at metabolic branch point. Mol. Microbiol. 92**,** 356-68.
Larner, J., 2002. D-*chiro*-inositol–its functional role in insulin action and its deficit in insulin resistance. Int. J. Exp. Diabetes Res. 3**,** 47-60.
Larner, J., Brautigan, D. L., Thorner, M. O., 2010. D-*chiro*-inositol glycans in insulin signaling and insulin resistance. Mol. Med. 16**,** 543-552.
Lim, H. N., Lee, Y., Hussein, R., 2011. Fundamental relationship between operon organization and gene expression. Proc. Natl. Acad. Sci. USA 108**,** 10626-10631.
Liu, X., Zhao, Z., Zhang, W., Sun, Y., Yang, Y., Bai, Z. J. E. i. l. s., 2017. Bicistronic expression strategy for high-level expression of recombinant proteins in *Corynebacterium glutamicum*. Eng. Life Sci. 17**,** 1118-1125.
Loewus, F. A., Murthy, P. P. N., 2000. *myo*-Inositol metabolism in plants. Plant Sci. 150**,** 1-19.
López-Gambero, A. J., Sanjuan, C., Serrano-Castro, P. J., Suárez, J., Rodríguez de Fonseca, F., 2020. The biomedical uses of inositols: A nutraceutical approach to metabolic dysfunction in aging and neurodegenerative diseases. Biomedicines 8**,** 295.
Monastra, G., Unfer, V., Harrath, A. H., Bizzarri, M., 2017. Combining treatment with *myo*-inositol and D-*chiro*-inositol (40: 1) is effective in restoring ovary function and metabolic balance in PCOS patients. Gynecol. Endocrinol. 33**,** 1-9.
Niebisch, A., Bott, M., 2001. Molecular analysis of the cytochrome bc_1-aa_3 branch of the *Corynebacterium glutamicum* respiratory chain containing an unusual diheme cytochrome c_1. Arch. Microbiol. 175**,** 282-294.
Ortmeyer, H. K., Bodkin, N., Lilley, K., Larner, J., Hansen, B. C., 1993. Chiroinositol deficiency and insulin resistance. I. Urinary excretion rate of chiroinositol is directly associated with insulin resistance in spontaneously diabetic rhesus monkeys. Endocrinology 132**,** 640-645.
Pintaudi, B., Di Vieste, G., Bonomo, M., 2016. The effectiveness of *myo*-inositol and D-*chiro*-inositol treatment in type 2 diabetes. Int. J. Endocrinol. 2016**,** 9132052.
Pupel, P., Szablińska-Piernik, J., Lahuta, L. B., 2019. Two-step D-ononitol epimerization pathway in *Medicago truncatula*. Plant J. 100**,** 237-250.
Ramp, P., Lehnert, A., Matamouros, S., Wirtz, A., Baumgart, M., Bott, M., 2021. Metabolic engineering of *Corynebacterium glutamicum* for production of *scyllo*-inositol, a drug candidate against Alzheimer's disease. Metab. Eng. 67**,** 173-185.
Ramp, P., Pfleger, C., Dittrich, J., Mack, C., Gohlke, H., Bott, M., 2022. Physiological, Biochemical, and Structural Bioinformatic Analysis of the Multiple Inositol Dehydrogenases from Corynebacterium glutamicum. Microbiol. Spectr. 10**,** e0195022.

Sanchez-Hidalgo, M., Leon-Gonzalez, A. J., Galvez-Peralta, M., Gonzalez-Mauraza, N. H., Martin-Cordero, C., 2021. D-Pinitol: A cyclitol with versatile biological and pharmacological activities. Phytochem. Rev. 20**,** 211-224.

Schäfer, A., Tauch, A., Jäger, W., Kalinowski, J., Thierbach, G., Pühler, A., 1994. Small mobilizable multi-purpose cloning vectors derived from the *Escherichia coli* plasmids pK18 and pK19: selection of defined deletions in the chromosome of *Corynebacterium glutamicum*. Gene 145**,** 69-73.

Spaans, S. K., Weusthuis, R. A., Van Der Oost, J., Kengen, S. W., 2015. NADPH-generating systems in bacteria and archaea. Front. Microbiol. 6**,** 742.

Thomas, M. P., Mills, S. J., Potter, B. V., 2016. The "other" inositols and their phosphates: synthesis, biology, and medicine (with recent advances in *myo*-inositol chemistry). Angew. Chem. Int. Ed. 55**,** 1614-1650.

van der Rest, M. E., Lange, C., Molenaar, D., 1999. A heat shock following electroporation induces highly efficient transformation of *Corynebacterium glutamicum* with xenogeneic plasmid DNA. Appl. Microbiol. Biotechnol. 52**,** 541-545.

Vitale, S. G., Corrado, F., Caruso, S., Di Benedetto, A., Giunta, L., Cianci, A., D'Anna, R., 2021. *Myo*-inositol supplementation to prevent gestational diabetes in overweight non-obese women: bioelectrical impedance analysis, metabolic aspects, obstetric and neonatal outcomes – a randomized and open-label, placebo-controlled clinical trial. Int. J. Food. Sci. Nutr. 72**,** 670-679.

Wendisch, V. F., 2020. Metabolic engineering advances and prospects for amino acid production. Metab. Eng. 58**,** 17-34.

Wolf, S., Becker, J., Tsuge, Y., Kawaguchi, H., Kondo, A., Marienhagen, J., Bott, M., Wendisch, V. F., Wittmann, C., 2021. Advances in metabolic engineering of *Corynebacterium glutamicum* to produce high-value active ingredients for food, feed, human health, and well-being. Essays Biochem. 65**,** 197-212.

Yoshida, K.-I., Yamaguchi, M., Ikeda, H., Omae, K., Tsurusaki, K.-i., Fujita, Y., 2004. The fifth gene of the *iol* operon of *Bacillus subtilis*, *iolE*, encodes 2-keto-*myo*-inositol dehydratase. Microbiology 150**,** 571-580.

Yoshida, K.-I., Yamaguchi, M., Morinaga, T., Ikeuchi, M., Kinehara, M., Ashida, H., 2006. Genetic modification of *Bacillus subtilis* for production of D-*chiro*-inositol, an investigational drug candidate for treatment of type 2 diabetes and polycystic ovary syndrome. Appl. Environ. Microbiol. 72**,** 1310-1315.

Yoshida, K.-I., Yamaguchi, M., Morinaga, T., Kinehara, M., Ikeuchi, M., Ashida, H., Fujita, Y., 2008. *Myo*-inositol catabolism in *Bacillus subtilis*. J. Biol. Chem. 283**,** 10415-10424.

Table 1

Bacterial strains and plasmids used in this study

Strain or plasmid	Relevant characteristics	Source or reference
Strains		
E. coli		
DH5α	F$^-$ Φ80*dlac*Δ(*lacZ*)M15 Δ(*lacZYA-argF*) U169 *endA1 recA1 hsdR17* (r_K^- , m_K^+) *deoR thi-1 phoA supE44* λ^- *gyrA96 relA1*; strain used for cloning procedures	(Hanahan, 1983)
C. glutamicum		
MB001(DE3)	Derivative of the prophage-free strain MB001 with a chromosomally encoded *E. coli lacI* gene under control of its native promoter followed by the T7 RNA polymerase gene under control of the *lac*UV5 promoter	(Kortmann et al., 2015)
MB001(DE3)Δ*iol1*Δ*iol2* (referred to as Δ*iol1*Δ*iol2*)	Derivative of MB001(DE3) with deletion of the gene clusters cg0196-cg0212 (*iol1*) and cg3389-cg3392 (*iol2*) involved in inositol metabolism	(Ramp et al. 2021)
ΔIOL	Derivative of MB001(DE3)Δ*iol1*Δ*iol2* with the additional deletion of the putative inositol dehydrogenase gene *idhA3* (cg2313)	This work
ΔIOLΔ*qsuB*	Derivative of ΔIOL with deletion of *qsuB* (cg0502)	This work
ΔIOLΔcg2312	Derivative of ΔIOL with deletion of cg2312	This work
ΔIOLΔcg2716	Derivative of ΔIOL with deletion of cg2716	This work
ΔIOLΔcg2822	Derivative of ΔIOL with deletion of cg2822	This work
ΔIOLΔcg2917	Derivative of ΔIOL with deletion of cg2917	This work
ΔIOLΔISO	Derivative of ΔIOL with deletion of *qsuB* (cg0502), cg2312, cg2716, cg2822, and cg2917	This work
ΔIDH	MB001(DE3) derivative with deletion of the genes *oxiC*-cg3390-*oxiD*-*oxiE* (cg3389-cg3392), *iolG* (cg0204), *iolW* (cg0207), *idhA3* (cg2313), and *oxiB* (cg0211)	(Ramp et al., 2022)
ΔIDHΔISO	ΔIDH derivative with deletion of *iolH* (cg0205), cg0212, *qsuB* (cg0502), cg2312, cg2716, cg2822, and cg2917	This work
Plasmids		
pK19mobsacB	Kan^R; plasmid for allelic exchange in *C. glutamicum*; (pK18 *ori*V$_{E.c.}$, *sacB*, *lacZ*α)	(Schäfer et al., 1994)

pK19mobsacB-Δ*qsuB*	pK19mobsacB derivative with 1000 bp homologous flanks upstream and downstream of cg0502	(Kallscheuer et al., 2016)
pK19mobsacB-Δcg2313	pK19mobsacB derivative with 1000 bp homologous flanks upstream and downstream of cg2313	This work
pK19mobsacB-Δcg0212	pK19mobsacB derivative with 1000 bp homologous flanks upstream and downstream of cg0212	This work
pK19mobsacB-Δcg2312-13	pK19mobsacB derivative with 1000 bp homologous flanks upstream and downstream of cg2312-2313	This work
pK19mobsacB-Δcg2716	pK19mobsacB derivative with 1000 bp homologous flanks upstream and downstream of cg2716	This work
pK19mobsacB-Δcg2822	pK19mobsacB derivative with 1000 bp homologous flanks upstream and downstream of cg2822	This work
pK19mobsacB-Δcg2917	pK19mobsacB derivative with 1000 bp homologous flanks upstream and downstream of cg2917	This work
pPREx6	Kan^R; pPREx2 derivative with P_{tac} exchanged for $P_{T7\text{-}lac}$ promoter	(Ramp et al., 2022)
pPREx6-IolH	Kan^R; pPREx6 derivative containing the *iolH* gene under control of P_{T7} and fused to a Strep-tag II sequence	This work
pPREx6-Cg0212	Kan^R; pPREx6 derivative containing the cg0212 gene under control of P_{T7} and fused to Strep-tag II sequence	This work
pPREx6-Cg3390	Kan^R; pPREx6 derivative containing the cg3390 gene under control of P_{T7} and fused to Strep-tag II sequence	This work
pMKEx2	Kan^R; *E. coli-C. glutamicum* shuttle vector (*lacI*, P_{T7}, lacO1, pHM1519 ori $_{Cg}$; pACYC177 ori $_{Ec}$) for expression of target genes under control of the T7 promoter	(Kortmann et al., 2015)
pIolG	pMKEx2 derivative for overexpression of *iolG* (cg0204)	(Ramp et al., 2022)
pCg0212	pMKEx2 derivative for overexpression of cg0212	This work
pIolG-cg0212	pMKEx2 derivative for overexpression of *iolG* (cg0204) and cg0212 in a synthetic operon	This work
pIolG-iolH	pMKEx2 derivative for overexpression of *iolG* (cg0204) and *iolH* (cg0205) in a synthetic operon	This work
pIolG-cg2312	pMKEx2 derivative for overexpression of *iolG* (cg0204) and cg2312 in a synthetic operon	This work
pIolG-cg2716	pMKEx2 derivative for overexpression of *iolG* (cg0204) and cg2716 in a synthetic operon	This work
pIolG-cg2822	pMKEx2 derivative for overexpression of *iolG* (cg0204) and cg2822 in a synthetic operon	This work
pIolG-cg2917	pMKEx2 derivative for overexpression of *iolG* (cg0204) and cg2917 in a synthetic operon	This work

pIolG-qsuB	pMKEx2 derivative for overexpression of *iolG* (cg0204) and *qsuB* (cg0502) in a synthetic operon	This work
pOEPa	pMKEx2 derivative for overexpression of the *MtOEPa* gene from *Medicago truncatula* codon-optimized for *C. glutamicum*	This work
pOEPb	pMKEx2 derivative for overexpression of the *MtOEPb* gene from *Medicago truncatula* codon-optimized for *C. glutamicum*	This work
pOEPa-b	pMKEx2 derivative for overexpression of *MtOEPa* and *MtOEPb* in a synthetic operon	This work
pOEPb-a	pMKEx2 derivative for overexpression of *MtOEPb* and *MtOEPa* in a synthetic operon	This work
pIno	pMKEx2 derivative for overexpression of *ino1*	This work
pInoDCI	pMKEx2 derivative for overexpression of *ino1*, *MtOEPa* and *MtOEPb* in a synthetic operon	This work
pETDuet-1	Amp^R; pBR322 *ori*; pET vector with two divergent T7 promoters	Novagen
pMKEx2-BiT7	pMKEx2 derivative containing two T7 promoters, *lacO* sites, MCSs and T7 terminators in opposite direction	This work
pBiT7-InoDCI	pMKEx2-BiT7 containing *ino1* under control of T7-1 and *MtOEPa* and *MtOEPb* in a synthetic operon under control of T7-2	This work

571

572

573 **Table 2**

574 *C. glutamicum* ATCC 13032 proteins belonging to the xylose isomerase-like superfamily in the InterPro

575 database.

Protein name	Locus tag	Accession number	Annotation
IolE	cg0203	Q8NTY8	2-keto-*myo*-inositol dehydratase
IolH	cg0205	Q8NTY6	sugar phosphate isomerases/epimerases
-	cg0212	Q8NTX9	putative phosphate isomerase/epimerase
QsuB	cg0502	Q8NT86	3-dehydroshikimate dehydratase
-	cg2312	Q8NNS8	putative hydroxypyruvate isomerase
Hyi	cg2716	Q8NMU3	hydroxypyruvate isomerase
-	cg2822	Q8NML9	putative sugar phosphate isomerase
-	cg2917	Q8NME4	conserved hypothetical protein
-	cg3390	Q8NL87	putative sugar phosphate isomerase

576

577

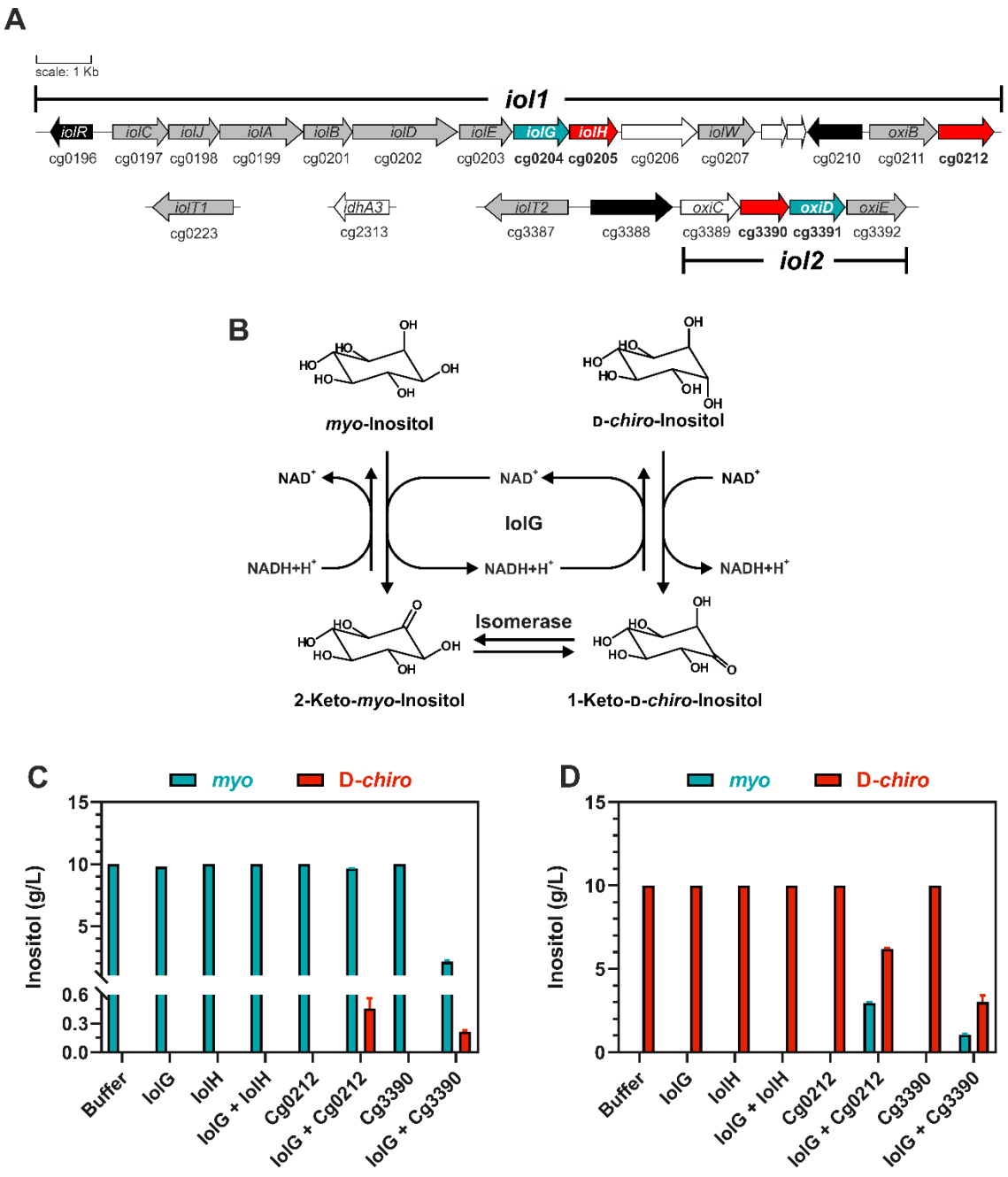

Fig. 1. Genes related to inositol metabolism in *C. glutamicum* and *in vitro* enzymatic interconversion of DCI and MI with purified enzymes. (A) Genes shown in black encode transcriptional regulators, genes in grey have a known or predicted function, and genes in white have putative or unknown functions. The genes *iolG* and *oxiD* encoding IDHs with activity for MI and DCI are shown in blue. Genes annotated as putative sugar phosphate isomerases (*iolH*, cg0212, cg3390) and tested for inosose isomerase activity are highlighted in red. (B) Scheme of the reversible NAD^+/NADH-dependent interconversion of MI and DCI catalyzed by IolG and an inosose isomerase. (C) *In vitro* enzymatic interconversion of DCI and MI with purified enzymes IolG, IolH, Cg0212, and Cg3390 starting from MI. (D) Same *in vitro* reaction starting from DCI. 50 µg of the indicated proteins were applied in a 200 µL buffered reaction mixture

592 containing 5 mM NAD^+ that was incubated at 30 °C for 24 h. Enzymatic activity was stopped
593 by heating at 80°C for 15 min and the inositol content was measured afterwards. Mean values
594 from technical triplicates and standard deviations are shown.
595

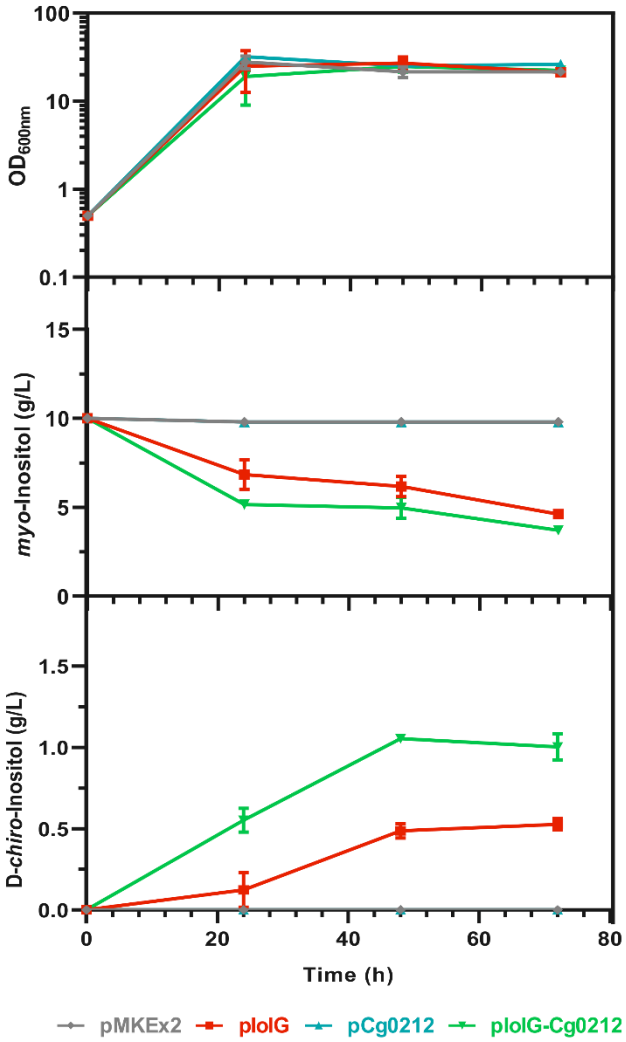

596

597 **Fig. 2.** Production of DCI from MI with *C. glutamicum* MB001(DE3)ΔIOL expressing *iolG*
598 and cg0212 in CGXII medium containing 20 g/L glucose and 10 g/L MI. Gene expression was
599 induced by addition of 500 µM IPTG at the cultivation start. Mean values of biological
600 triplicates and standard deviations are shown.

601

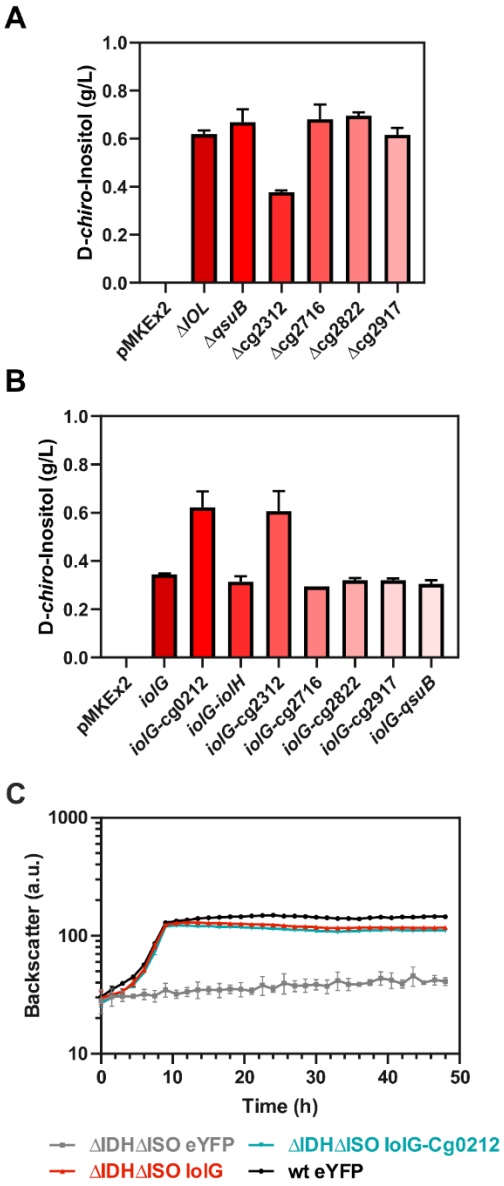

Fig. 3. Impact of putative inosose isomerases on DCI production from MI and on growth with DCI as sole carbon source. (A) Final DCI titer of *C. glutamicum* MB001(DE3)ΔIOL expressing *iolG* with pIolG and derivatives with either *qsuB*, cg2312, cg2716, cg2822, or cg2917 deleted. (B) Final DCI titer of *C. glutamicum* MB001(DE3)ΔIOLΔISO expressing *iolG* alone or together with a putative inosose isomerase gene as a synthetic operon in pMKEx2. The strains were cultivated in CGXII medium containing 20 g/L glucose and 10 g/L MI for 72 h at 30°C. Gene expression was induced by the addition of 500 µM IPTG at the start of the cultivation. Mean values of biological triplicates and standard deviations are shown. (C) Growth on DCI of *C. glutamicum* ΔIDHΔISO expressing *iolG* alone or in combination with the inosose isomerase gene cg0212 or as negative control *eyfp* using the corresponding pMKEx2-based plasmids. *C. glutamicum* MB001(DE3) transformed with pMKEx2-eyfp was used as a positive control. The strains were cultivated in a BioLector system using CGXII minimal medium containing 10 g/L DCI as sole carbon and energy source. The cultures were incubated for 48 h at 30 °C, 1200 rpm, and 85% humidity. Mean values and standard deviations of three biological replicates are shown.

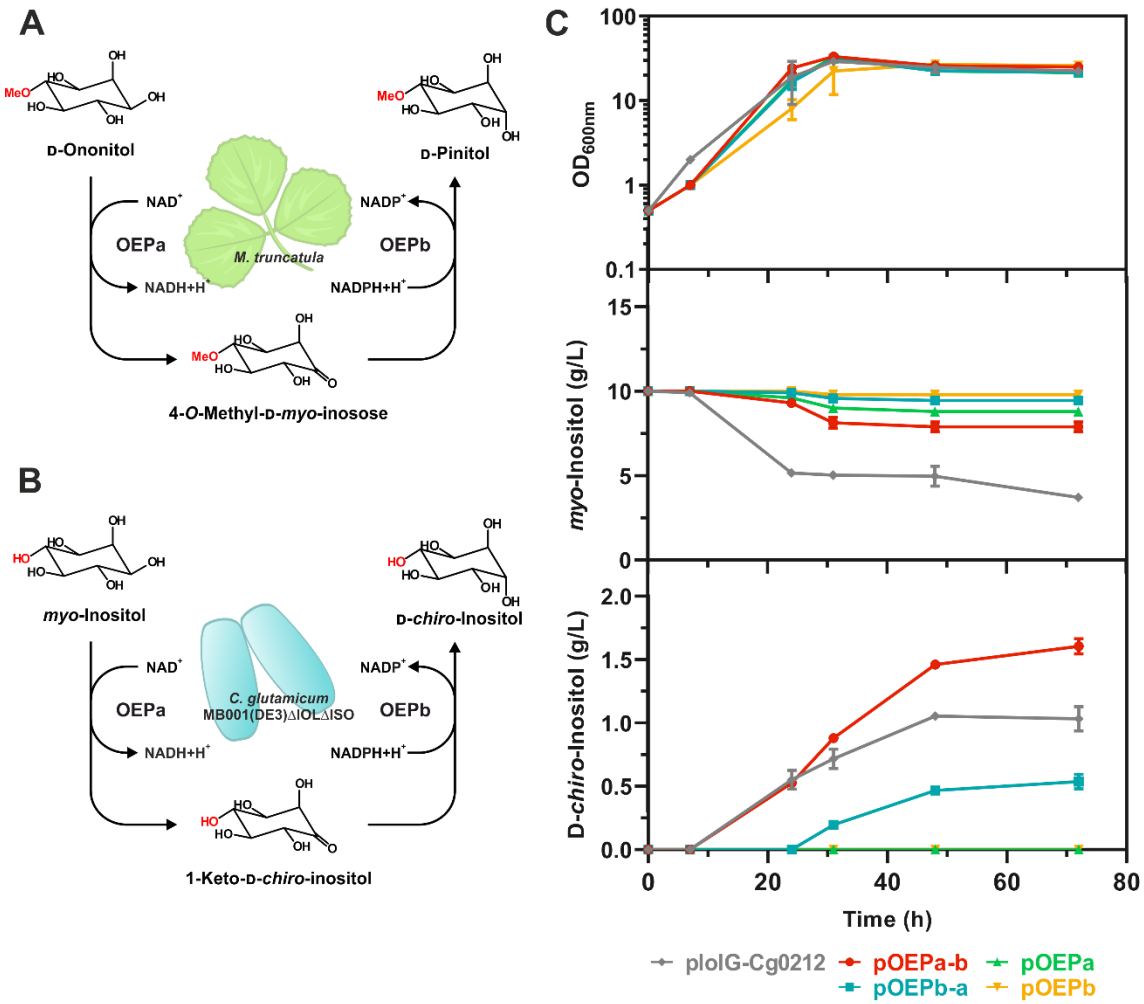

Fig. 4. (A) Scheme of natural D-pinitol (4-*O*-methyl-D-*chiro*-inositol) biosynthesis from D-ononitol (4-*O*-methyl-*myo*-inositol) in barrelclover *(Medicaco truncatula)* catalyzed by the NAD^+-dependent D-ononitol dehydrogenase MtOEPa and the $NADP^+$-dependent D-pinitol dehydrogenase MtOEPb. (B) Scheme of the predicted DCI production from MI by the promiscuous activity of MtOEPa and MtOEPb expressed in *C. glutamicum* MB001(DE3)ΔIOLΔISO. (C) Growth, MI consumption, and DCI production of *C. glutamicum* MB001(DE3)ΔIOLΔISO containing pMKEx2-derived plasmids for expression of the *MtOEPa* and *MtOEPb* genes either together in different order (pOEPa-b, pOEPb-a) or alone (pOEPa, pOEPb). For comparison, strain MB001(DE3)ΔIOL pIolG-Cg0212 was analyzed. Gene expression was induced by addition of 500 µM IPTG at the start of the cultivation. Mean values of biological triplicates and standard deviations are shown.

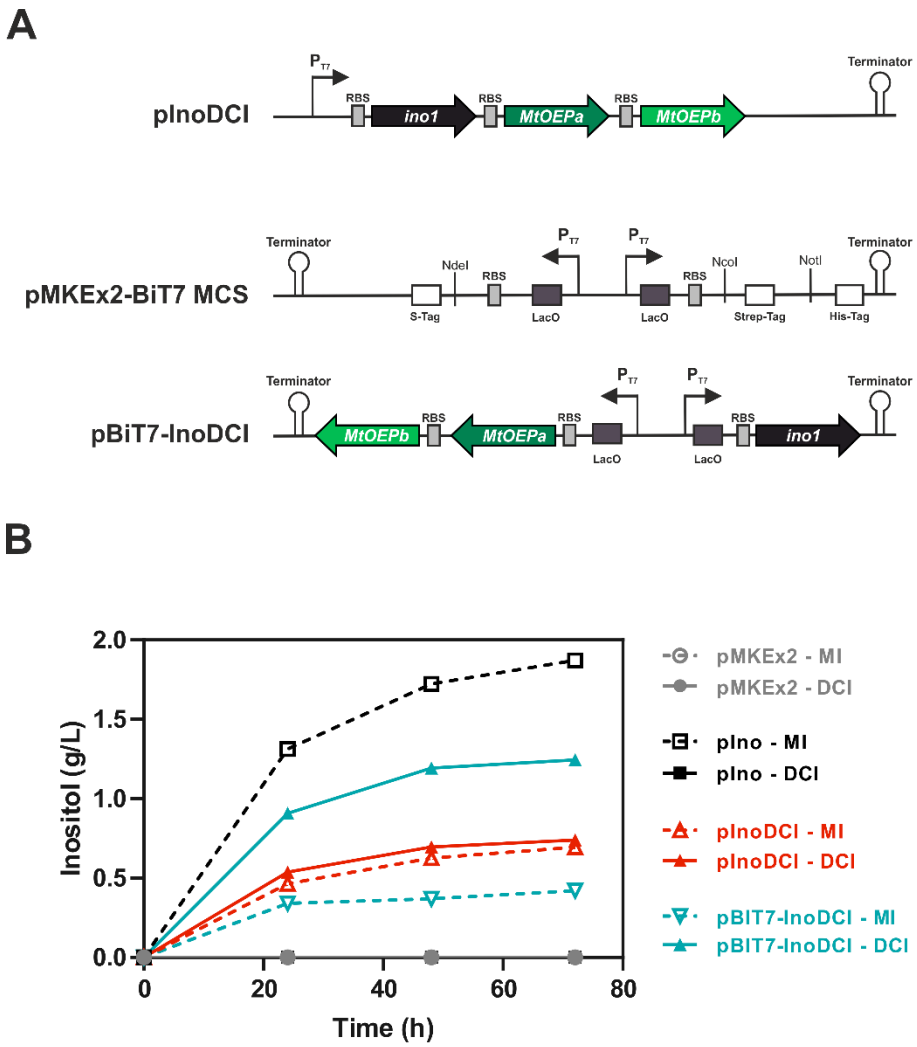

Fig. 5. Synthetic operons for DCI production from glucose. (A) Scheme of the expression cassette of pInoDCI (one operon), the cloning sites in the newly constructed expression vector pMKEx2-BiT7, and the bicistronic expression cassette of pBiT7-InoDCI. (B) Production of DCI and MI from glucose by expressing the dehydrogenase genes *MtOEPa* and *MtOEPb* together with *ino1* in two different expression cassettes or *ino1* alone in *C. glutamicum* MB001(DE3)ΔIOLΔISO. Strains were cultivated in CGXII medium containing 20 g/L glucose for 72 h at 30 °C. Gene expression was induced by addition of 500 µM IPTG 3 h after the start of the cultivation. Mean values of biological triplicates and standard deviations are shown.

Supplementary Information

Alternative routes for production of the drug candidate D-*chiro*-inositol with *Corynebacterium glutamicum* using endogenous or promiscuous plant enzymes

Paul Ramp, Christina Mack, Astrid Wirtz, Michael Bott[#]

IBG-1: Biotechnology, Institute of Bio- and Geosciences, Forschungszentrum Jülich, Jülich, Germany

[#]Corresponding author: m.bott@fz-juelich.de

Table S1

Oligonucleotides used in this study

Oligonucleotide name	Oligonucleotide sequence (5'→ 3')
pK19mobsacB plasmids	
P01_pK19Δcg2313_FW1	GAGGATCCCCGGGTACCGAGCTCGCCTCAAGCGGAACCTGAAG
P02_pK19Δcg2313_RV1	CTTGCTGAAAGCATCGAGG
P03_pK19Δcg2313_FW2	GTTAAACCTCGATGCTTTCAGCAAGGAGGGCAAGTTTGACTGAC
P04_pK19Δcg2313_RV2	CGTTGTAAAACGACGGCCAGTGAATTATGGTGGTCAAGCCGATG
P05_pK19Δcg0212_FW1	GCATGCCTGCAGGTCGACTCTAGAGTCGTGGTGGCTAACTTCCTG
P06_pK19Δcg0212_RV1	TTTAAGAAACCAGGGACTCTTCGAGGTTGTAGAGACCGAGTTTCATG
P07_pK19Δcg0212_FW2	CACCATGAAACTCGGTCTCTACAACCTCGAAGAGTCCCTGGTTTC
P08_pK19Δcg0212_RV2	GTTGTAAAACGACGGCCAGTGAATTAGATCCTTGGTCACCAGATC
P09_pK19Δcg2312-13_FW1	GAGGATCCCCGGGTACCGAGCTCGGAATCTGACTCCGAGCAG
P10_pK19Δcg2312-13_RV1	AAGTCAGCGTTCACGGTC
P11_pK19Δcg2312-1313_FW2	ATTTAGACCGTGAACGCTGACTTGAGGGCAAGTTTGACTGAC
P12_pK19Δcg2312-1313_RV2	CGTTGTAAAACGACGGCCAGTGAATTATGGTGGTCAAGCCGATG
P13_pK19Δcg2716_FW1	ATGCCTGCAGGTCGACTCTAGAGAGTCAGCCATGCATCTAC
P14_pK19Δcg2716_RV1	GGCAGCAAATCGAGACAAG
P15_pK19Δcg2716_FW2	TCTTATCTTGTCTCGATTTGCTGCCGGCTGGTTGGAGCTCTAG
P16_pK19Δcg2716_RV2	GTAAAACGACGGCCAGTGAATTACGATCACGTGGCGCTTC
P17_pK19Δcg2822_FW1	ATGCCTGCAGGTCGACTCTAGAGATAGATTGTTTAGGCCGTGAAAAGC
P18_pK19Δcg2822_RV1	AATTCCTGCGGCATCCAATTTGGC
P19_pK19Δcg2822_FW2	GCCAAATTGGATGCCGCAGGAATTAACGCCGAGTACAACTAAG
P20_pK19Δcg2822_RV2	GTAAAACGACGGCCAGTGAATTGTGTGAATTACTTTGCAACGC
P21_pK19Δcg2917_FW1	ATGCCTGCAGGTCGACTCTAGAGGAGGGTCCAGTGTTCTTG
P22_pK19Δcg2917_RV1	AACGATGGGGAAGTAGCC
P23_pK19Δcg2917_FW2	GAGAGGCTACTTCCCCATCGTTTGCGAGGCGCACTAGTTGATC
P24_pK19Δcg2917_RV2	GTAAAACGACGGCCAGTGAATTAAAGCATCGGAAACCGCAG
Recombination analysis	
P25_ΔCg2313_FW	GTTCCATCAAAGTCAATGC
P26_ΔCg2313_RV	GTGCGCCGTGTGATCAATG
P27_ΔQsuB_FW	CACTGGCGATGACCTTG
P28_ΔQsuB_RV	GAGACGTCGGTGTTGTG
P29_Δcg2312_FW	GGAATGGGCTGCGTTG
P30_Δcg2312_RV	GCAGAAGTTTCGGTGTG
P31_Δcg2716_FW	ATCCACCAATGCTGACAC
P32_Δcg2716_RV	AGGTTAGCGTCAGTGAC
P33_Δcg2822_FW	CAAGCTCCGGTTTCAGCG
P34_Δcg2822_RV	GTGTGAATTACTTTGCAACGC
P35_Δcg2917_FW	ATTTGCGCACGAAGGTGG
P36_Δcg2917_RV	CGCAATCGCACTGTCTG
pPREx6 plasmids	
P37_px6-IolH_FW	AGAAGGAGATATACATATGAACGTGGTTCGTATTG
P38_px6-IolH_FW	TGGGTGGGACCAGCTAGCTGCGTTTTCGATGAGTG

P39_px6-Cg0212_FW	TTAACTTTAAGAAGGAGATATACATATGAAACTCGGTCTCTAC
P40_px6-Cg0212_FW	CGAACTGTGGGTGGGACCAGCTAGCAGAAACCAGGGACTCTTC
P41_px6-Cg3390_FW	AGAAGGAGATATACATATGAAACCACAACTTATTG
P42_px6-Cg3390_FW	GGTGGGACCAGCTAGCGTTAGTGGAGGGGGCG
pMKEx2 plasmids	
P43_pCg0212_FW	CTTTAAGAAGGAGATATACCATGAAACTCGGTCTCTAC
P44_pCg0212_RV	GCACCAGAGCGAGCTCTGCGGCCGCTTAAGAAACCAGGGACTC
P45_pIolG-Cg0212_FW1	CTTTAAGAAGGAGATATACCATGAGCAAGAGCCTTCGCGTTGG
P46_pIolG-Cg0212_RV1	TGTCGCTCAGAGACCTGAGGTTAAGCGTAGAAATCTGGGCGAG
P47_pIolG-Cg0212_FW2	CCTCAGGTCTCTGAGCGACAGAAGGAGATATACCATGAAACTCGGTCTCTAC
P48_pIolG-Cg0212_RV2	GCACCAGAGCGAGCTCTGCGGCCGCTTAAGAAACCAGGGACTC
P49_pIolG-Cg2312_FW	CCTCAGGTCTCTGAGCGACAGAAGGAGATATACCATGACTTTTAAACTCGCAGC
P50_pIolG-Cg2312_RV	CCAGAGCGAGCTCTGCGGCCTTAGACCGTGAACGCTGAC
P51_pIolG-IolH_FW	CCTCAGGTCTCTGAGCGACAGAAGGAGATATACCATGAACGTGGTTCGTATTGC
P52_pIolG-IolH_RV	CCAGAGCGAGCTCTGCGGCCCTATGCGTTTTCGATGAGTG
P53_pIolG-Cg2716_FW	CCTCAGGTCTCTGAGCGACAGAAGGAGATATACCATGTCTCGATTTGCTGCCAAC
P54_pIolG-Cg2716_RV	CCAGAGCGAGCTCTGCGGCCCTAGAGCTCCAACCAGCC
P55_pIolG-Cg2822_FW	CCTCAGGTCTCTGAGCGACAGAAGGAGATATACCATGGATGCCGCAGGAATTTC
P56_pIolG-Cg2822_RV	CCAGAGCGAGCTCTGCGGCCTTAGTTGTACTCGGCGTTG
P57_pIolG-Cg2917_FW	CCTCAGGTCTCTGAGCGACAGAAGGAGATATACCATGCGCCTCGCAGCTGCCAC
P58_pIolG-Cg2917_RV	CCAGAGCGAGCTCTGCGGCCCATTTAGACTGCTTCCTCAATTTTTTC
P59_pIolG-QsuB_FW	CCTCAGGTCTCTGAGCGACAGAAGGAGATATACCATGATGCGTACATCCATTGCCAC
P60_pIolG-QsuB_RV	CCAGAGCGAGCTCTGCGGCCCTAGTTTGGGATTCCCCGC
P61_pOEPa_FW	CCTCAGGTCTCTGAGCGACAGAAGGAGATATACCATGTCCAAGACCGTGTGC
P62_pOEPa_RV	TGGCACCAGAGCGAGCTCTGCGGCCTTACACCAGGCCACGGGACTTC
P63_pOEPb_FW	TTTAACTTTAAGAAGGAGATATACCATGGCAGGCAACAAGATCCC
P64_pOEPb_RV	TGGCACCAGAGCGAGCTCTGCGGCCTTACACGTCGCCATCCCAC
P65_pOEPa-b_FW	GCAGGTGCACAATGATACGATTACACCAGGCCACGGGAC
P66_pOEPa-b_RV	TCGTATCATTGTGCACCTGCGAAGGAGATATACCATGGCAGGCAACAAGATCCC
P67_pOEPb-a_FW	GCAGGTGCACAATGATACGATTACACGTCGCCATCCCACAGTTC
P68_pOEPb-a_RV	TCGTATCATTGTGCACCTGCGAAGGAGATATACCATGTCCAAGACCGTGTGCG
P69_pInoDCI_FW1	CTTTAAGAAGGAGATATACCATGAGCACGTCCACCATCAG
P70_pInoDCI_RV	ACATCGTTGAGTGGTCACCGTTACGCCTCGATGATGAATG
P71_pInoDCI_FW2	CGGTGACCACTCAACGATGTGAAGGAGATATACCATGTCCAAGACCGTG
P72_pMKEx2-BiT7_FW1	TCGGGCTCATGAGCGCTTGTTTCGGTAATCGTATTGTACACGGCCG
P73_pMKEx2-BiT7_RV1	CGGCCACGGGGCCTGCCACCATACATCCGGATATAGTTCCTCC
P74_pMKEx2-BiT7_RV2	CCGAAACAAGCGCTCATG
P75_pMKEx2-BiT7_FW2	TCGCAGACCGATACCAGGATCTTG
P76_pMKEx2-BiT7_RV3	TCACCGAGGCAGTTCCATAGGATGG
P77_pMKEx2-BiT7_FW3	GTATGGTGGCAGGCCCCGTG
P78_pBiT7-InoDCI_FW1	GCACCAGAGCGAGCTCTGCGGCCTTACGCCTCGATGATGAATG
P79_pBiT7-InoDCI_RV1	GTTAAGTATAAGAAGGAGATATACAATGTCCAAGACCGTGTGC
P80_pBiT7-InoDCI_RV2	CGATATCCAATTGAGATCTGCCATATTACACGTCGCCATCCCAC

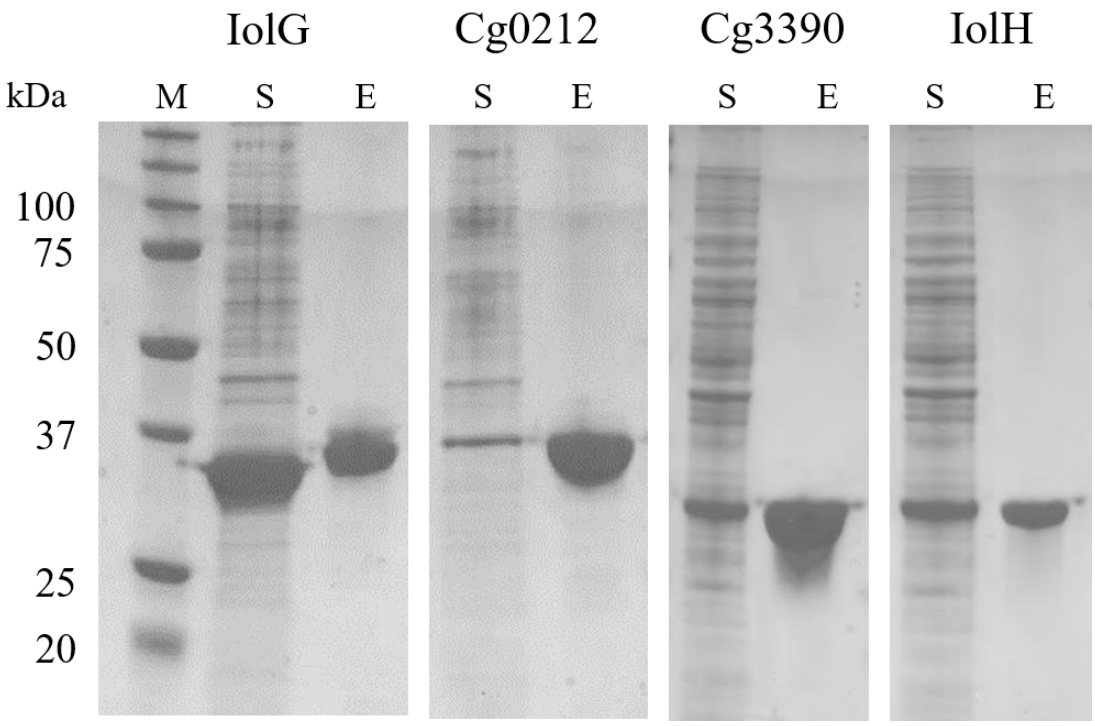

Fig. S1. Coomassie-stained SDS-polyacrylamide gels of purified IolG, Cg0212, Cg3390 and IolH. Shown are supernatant fractions of lysed *C. glutamicum* cells overexpressing the mentioned proteins (S) and final elution fractions (E) after purification by StrepTactin-Sepharose affinity chromatography and size-exclusion chromatography.

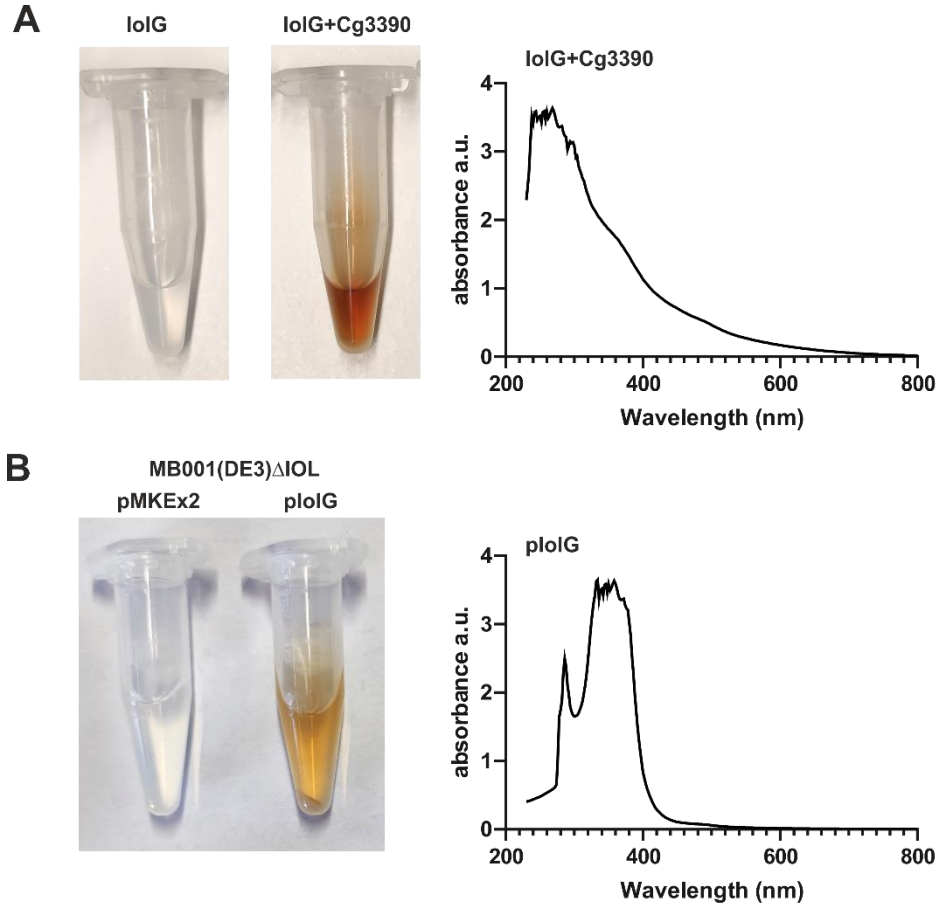

Fig. S2. Coloration caused by inositol metabolization by IolG and Cg3390. (A) Samples of an *in vitro* reaction mixture (200 µl) containing MI (10 g/L), NAD^+ (5 mM) and purified IolG or IolG combined with purified Cg3390 (50 µg each) that was incubated for 24 h at 30 °C. The UV-VIS spectrum (230 – 800 nm) of the sample containing Cg3390 is shown at the left and was corrected for absorption of the buffer used. (B) Culture supernatant of *C. glutamicum* MB001(DE3)ΔIOL transformed with pMKEx2 or pIolG and cultivated in CGXII medium with 20 g/L glucose and 10 g/L MI at 30 °C for 48 h. The UV-VIS spectrum (230 – 800 nm) of the colored supernatant is shown at the left and was corrected for absorption of CGXII medium.